BJR

Received:
9 October 2015

Accepted:
11 November 2015

doi: 10.1259/bjr.20150851

Cite this article as:
Offiah CE, Dean J. Post-mortem CT and MRI: appropriate post-mortem imaging appearances and changes related to cardiopulmonary resuscitation. *Br J Radiol* 2016; **89**: 20150851.

REVIEW ARTICLE

Post-mortem CT and MRI: appropriate post-mortem imaging appearances and changes related to cardiopulmonary resuscitation

CURTIS E OFFIAH, FRCS, FRCR and JONATHAN DEAN, BSc

Department of Radiology and Imaging, Royal London Hospital, Barts Health NHS Trust, London, UK

Address correspondence to: Dr Curtis E Offiah
E-mail: *curtis.offiah@bartshealth.nhs.uk*

ABSTRACT

Post-mortem cross-sectional imaging in the form of CT and, less frequently, MRI is an emerging facility in the evaluation of cause-of-death and human identification for the coronial service as well as in assisting the forensic investigation of suspicious deaths and homicide. There are marked differences between the radiological evaluation and interpretation of the CT and MRI features of the live patient (*i.e.* antemortem imaging) and the evaluation and interpretation of post-mortem CT and MRI appearances. In addition to the absence of frequently utilized tissue enhancement following intravenous contrast administration in antemortem imaging, there are a number of variable changes which occur in the tissues and organs of the body as a normal process following death, some of which are, in addition, affected significantly by environmental factors. Many patients and victims will also have undergone aggressive attempts at cardiopulmonary resuscitation in the perimortem period which will also significantly alter post-mortem CT and MRI appearances. It is paramount that the radiologist and pathologist engaged in the interpretation of such post-mortem imaging are familiar with the appropriate non-pathological imaging changes germane to death, the post-mortem interval and cardiopulmonary resuscitation in order to avoid erroneously attributing such changes to trauma or pathology. Some of the more frequently encountered radiological imaging considerations of this nature will be reviewed.

INTRODUCTION

Post-mortem cross-sectional imaging assessment in the form of CT and, less frequently, MRI has become an emerging phenomenon in the UK to assist the coronial service in identifying the cause of death non-invasively in individuals where circumstances are non-suspicious or non-homicidal but where appropriate recent medical history is not available. Such imaging has also become a versatile addition to the armoury available to the forensic pathologist and crime scene investigating (police) authorities in the evaluation of suspicious and homicidal causes of death.

It has become increasingly evident that the imaging interpretation of post-mortem CT and MRI is very different to antemortem cross-sectional imaging assessment. There are a number of tissue changes which occur post-mortem and impact significantly on the CT and MRI appearances. Experience of these changes is crucial to avoid erroneous imaging interpretation. Similarly, the effects of perimortem cardiopulmonary resuscitation can cause a number of changes which may be evident on subsequent post-mortem imaging and should not be misinterpreted as pathological or non-iatrogenic. We present a review of appropriate post-mortem CT and MRI changes as well as iatrogenic changes related to perimortem cardiopulmonary resuscitation. Cases will be drawn from the coronial workload undertaken. Imaging undertaken for the forensic pathology service and subsequent criminal investigation will not be presented.

POST-MORTEM CHANGES

Changes in tissue imaging appearances with temperature

Cessation of the body's normal thermogenic metabolism at death results in a gradual decrease in body temperature to ambient temperature. In addition, storage of the body in the mortuary involves refrigeration at approximately 4 °C; some mortuary facilities also incorporate freezer compartments for longer-term storage. Although CT appearances are not as prone to changes with such refrigeration cooling effects, MRI sequences are sensitive to temperature. An understanding of these potential temperature effects on MRI are advantageous even though, currently, the majority of post-mortem cross-sectional imaging undertaken for coronial and forensic assessment (particularly for adult cases) utilizes CT imaging.[1,2]

Figure 1. (a) Coronal fluid-attenuated inversion recovery (FLAIR) image utilizing a typical (antemortem) inversion time of 2000 ms at which nulling of the water signal normally occurs in the living subject. On this post-mortem sequence of a cooled subject, the cerebrospinal fluid (CSF) fails to suppress. (b) Coronal FLAIR image of the same post-mortem study as in (a) but with an inversion time of 1200 ms utilized. The CSF has now suppressed satisfactorily.

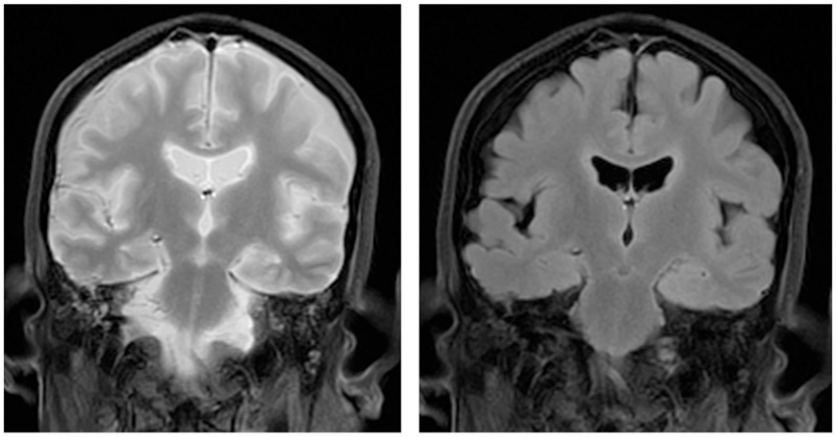

(a) (b)

(1) *Altered cerebrospinal fluid signal intensity on fluid-attenuated inversion recovery sequences*: there is a direct relationship between temperature and the T_1 value of cerebrospinal fluid (CSF) such that a decrease in temperature results in a fall in T_1 and, as a consequence, the inversion time to suppress the CSF signal is shortened on fluid-attenuated inversion recovery sequences when body temperature is low. CSF signal therefore may appear high on fluid-attenuated inversion recovery images (Figure 1a). This can be suppressed by shortening the inversion time (Figure 1b).[3–6]
(2) *Altered signal intensity of fat on T_2 weighted sequences*: when body temperature decreases, the T_2 value of fat is decreased in a linear fashion, whereas the T_1 value is initially shortened and then subsequently prolonged. As a result, the signal intensity of fat is suppressed on T_2 weighted imaging when the body temperature is low (Figure 2).[3,5]
(3) *Altered signal intensity of frozen tissues on T_1 weighted and T_2 weighted sequences*: when tissue temperature decreases to freezing point, the T_1 value is markedly prolonged and the T_2 value is markedly shortened resulting in a low signal intensity of frozen tissues on both T_1 weighted and T_2 weighted images.[3,6]
(4) *Altered apparent diffusion coefficient*: altered apparent diffusion coefficient (ADC) values are reduced (and b1000 values increased) globally across the brain parenchyma by low body temperature (Figure 3), but relative ADC values between

Figure 2. Axial T_2 weighted fast spin-echo sequence through the thorax of a post-mortem MRI study. The cooled post-mortem temperature of the subject (transferred from the mortuary to scanner without any significant delay) exhibits suppression of the normal high T_2 signal of fat—the subcutaneous fat exhibits low signal.

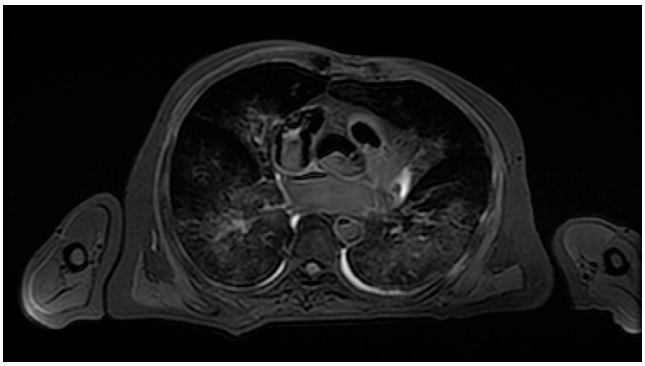

Figure 3. Axial apparent diffusion coefficient (ADC) of the brain of a post-mortem study. The cooled post-mortem brain exhibits globally reduced ADC signal throughout the parenchyma compared with typical antemortem signal appearances. However, the relative ADC signal throughout different parts of the brain remains the same as in the normal antemortem study.

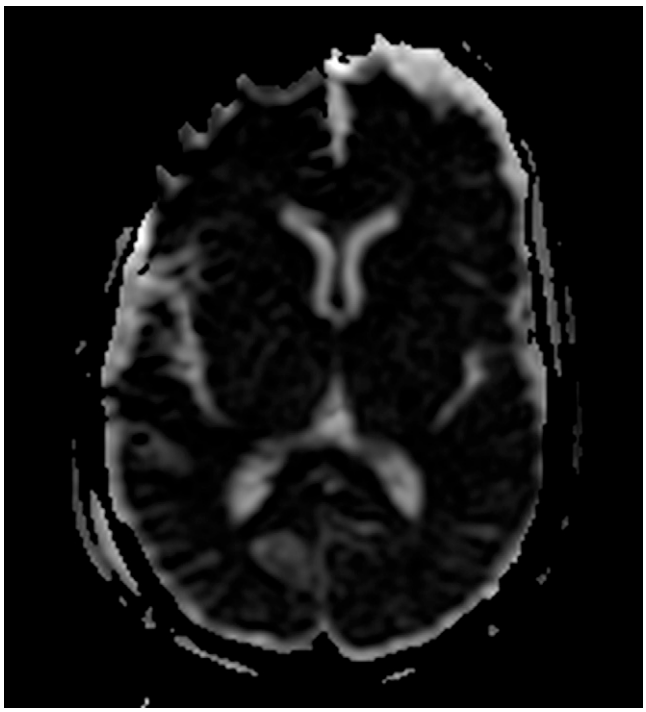

Figure 4. *Hypostasis*: (a) axial post-mortem CT image through the mediastinum of an elderly adult male demonstrates intravascular hypostasis with intraluminal fluid–fluid levels evident in the descending aorta and pulmonary trunk and arteries where erythrocytes have separated from serum and settled in the dependent parts of the vessels (arrows). (Note the bilateral pleural effusions present at the time of death.) (b) Axial post-mortem CT image through the thorax of the same subject with appropriate gradation of subtle increased attenuation in the dependent subcutaneous tissues (posterior in this case) (arrows) compared with the non-dependent subcutaneous tissues (anterior) and the associated subtle dependent dermal thickening (arrows).

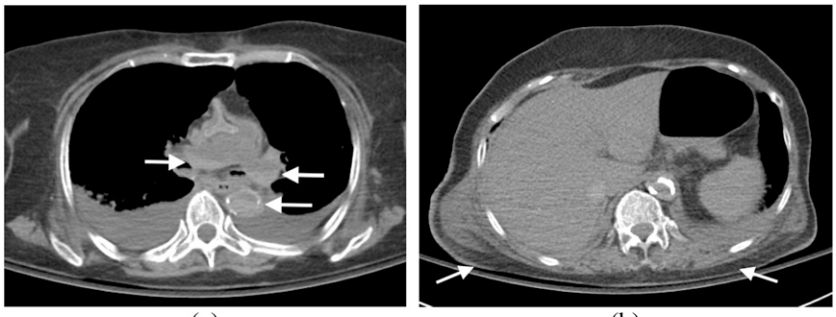

different parts of the brain (for example, white matter relative to grey matter) are preserved and therefore adjustment of window level and width settings can correct this change for qualitative evaluation.[3,7]

(5) *Altered attenuation of frozen tissue on CT*: the attenuation of a liquid component on CT depends on its density which varies with temperature. Water density remains almost constant between 0 °C and normal body temperature. Given that the human body comprises 70% water, the attenuation of the human tissue does not exhibit any discernible difference between 0 °C and normal body temperature. However, the density of ice is lower than the density of water and, as a result, there is visible difference in the CT attenuation characteristics of the human body in the frozen state compared with that above 0 °C. However, practically, this will rarely be evidenced on routine post-mortem CT imaging, as frozen cadavers are typically defrosted before any evaluation is undertaken by the pathologist and radiologist.

Hypostasis

Also termed livor mortis or lividity, hypostasis is the earliest post-mortem change and occurs throughout all tissues and organs of the body. With progression of the post-mortem period, livor mortis (hypostasis) will eventually become fixed and no longer position dependent. On post-mortem CT assessment, hypostasis is evident as increased attenuation of the affected organs, of the fluid containing compartments such as the vasculature and of the tissues. In large vessels such as the aorta, dural venous sinuses and cardiac chambers, this is particularly evident, with the blood separating into the serum and erythrocytes; the high attenuation erythrocytes form a separate dependent layer relative to the serum (Figure 4a). Intravascular sedimentation can occur within 2 h post-mortem.[8,9] This distribution of intravascular hyperdensity can be helpful in identifying pulmonary thromboembolic disease on post-mortem CT assessment with thrombus appearing as intraluminal conglomerate casts of hyperdensity in non-dependent parts of the vessel.

Within the viscera, hypostasis is most readily identified in the skin and in the lung parenchyma on post-mortem CT and MRI; a gradient of progressively increasing attenuation or signal variation, respectively, may be evident with transition from non-dependent to dependent parts of these organs[10] (Figure 4b and 5a,b). With hypostasis of the skin, there may also be subtle

Figure 5. *Hypostasis*: (a) axial post-mortem T_1 weighted sequence through the thorax of an adult male subject demonstrates post-mortem lung lividity in the dependent parts of the lung parenchyma with a gradient of mild signal change present in the posterior dependent parts of the lungs (arrows). (b) Axial post-mortem CT image on lung window settings through the thorax of an adult male subject with a mild gradient of increasing attenuation change from the non-dependent anterior aspects of the lungs (thin arrows) through to the dependent posterior aspects of the lungs (thick arrows).

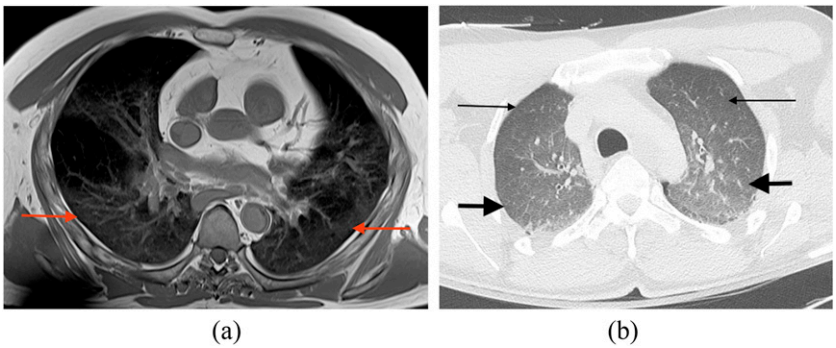

Figure 6. *Decomposition*: (a) axial post-mortem CT image of the brain of an adult male subject exhibits early decomposition change with cerebral autolysis present—there is rather "bland" attenuation of the brain parenchyma, loss of normally appreciable sulci and early putrefactive change with intravascular gas formation noted (arrows). (b) Axial post-mortem CT image of an adult female subject demonstrates more advanced putrefactive change with more extensive intravascular and extravascular intracranial gas and early brain parenchymal "settling".

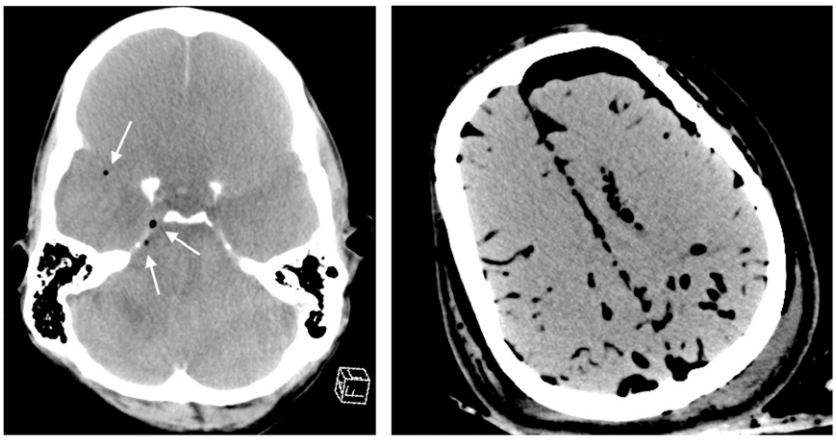

dermal thickening present in the dependent areas (Figure 4b). The post-mortem CT and MRI changes that may be present in the lungs as a result of pulmonary oedema or bronchopneumonia as well as those evident in the skin and subcutaneous tissues because of blunt trauma, for example, typically differ from these normal livor mortis features in distribution and severity of hyperattenuation and signal change.

Decomposition

This process occurs as a result of autolysis and putrefaction with the additional possibility of insect infestation and animal predation (consumption by animals). There are a number of factors which can affect the rate of decomposition: ambient temperature, humidity, body weight and size, clothing, the type of surface the body is resting on and the access of the body to insects and predatory animals. Eventually, there will be complete skeletonization of the body, but the degree of decomposition is also affected by the humidity and microbial environment present.[8,11]

Figure 7. *Decomposition*: Axial post-mortem CT image through the abdomen (on lung window settings) demonstrates marked post-mortem small and large bowel dilatation in a young male patient due to putrefactive gas formation. There is also putrefactive intravascular gas within the abdominal aorta (thick arrow) and inferior vena cava (thin arrow) as well as in relation to the paraspinal and paravertebral soft tissues.

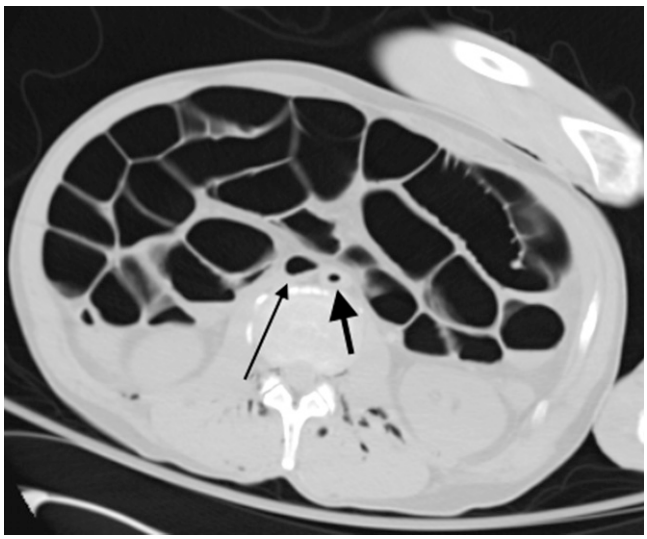

Figure 8. Sagittal oblique post-mortem T_2 fast spin-echo sequence through the mediastinum and heart. The right ventricle (short broken arrow) and ascending aorta (thin arrow) are indicated. A small amount of putrefactive pericardial fluid is present (large bold arrow) outlining the posterior aspect of the left ventricle. The normal high T_2 signal related to fat is suppressed owing to the post-mortem low body temperature.

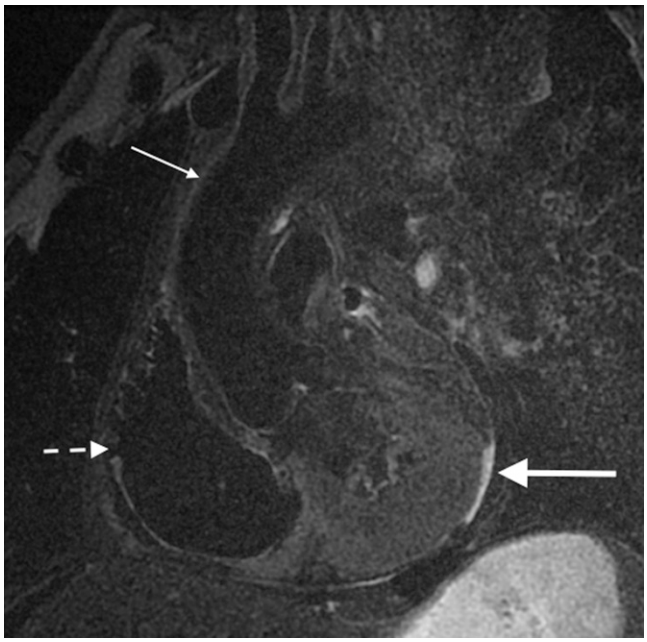

Figure 9. Axial post-mortem CT image through the upper abdomen demonstrates normal post-mortem decomposition putrefactive gas in the hepatic veins (arrow) (as well as in the abdominal aorta and inferior vena cava).

Arbitrarily, the extent of post-mortem decomposition changes on CT (and MRI) can be classified as early, moderate or advanced. The earliest changes appreciable on post-mortem imaging are usually in the brain, and on CT, include loss of grey–white matter differentiation, decreased attenuation and loss of sulcal definition (Figure 6a). These changes represent cerebral autolysis at a pathological level. Putrefaction also begins with gas appearing within the intracranial (extra-axial and intraparenchymal) vessels (Figure 6a). Eventually, the brain softens, and on post-mortem imaging, this is appreciated as "settling" of the brain parenchyma towards the dependent part of the cranium and gas accumulation in the non-dependent part of the cranium (Figure 6b); some of this gas may be putrefactive in origin. Finally, the brain liquefies and becomes water attenuation. The brain parenchymal decomposition changes are accompanied by loss of ocular volume in the late phase and the intraocular lenses may become both subluxed/detached as well as lose attenuation. It is imperative that these anticipated intracranial and intraorbital decomposition changes are appreciated as such and not erroneously attributed to trauma or air embolus, for example.

Figure 10. Axial post-mortem CT image through the superior mediastinum of an elderly male subject demonstrates mural hyperdensity of the ascending aorta (white arrows) which can be a normal appropriate post-mortem CT finding. There is also evidence of intravascular hypostasis in the ascending aorta (black thin arrow).

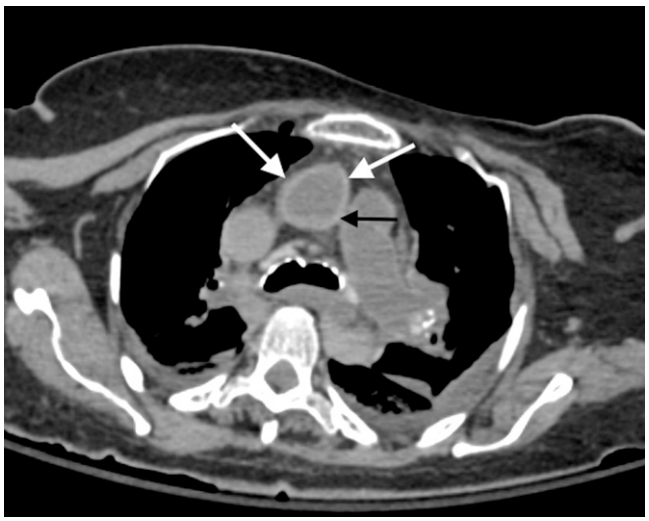

The intra-abdominal compartment is the first region to exhibit putrefactive changes of decomposition with gas evident in the intestinal wall and the mesenteric vessels and portal venous system; the small and large bowel become distended with putrefactive gases produced by the intestinal flora (Figure 7). A small amount of fluid accumulates in the pleural and peritoneal and pericardial cavities presumably as a consequence of putrefaction fluid from fat (Figure 8). Putrefactive intravascular gas eventually evolves (Figure 9). Appreciation of this phenomenon is vital in order to avoid misinterpreting such changes as pathological air embolus on imaging.

Adipocere is a waxy substance derived from body fat. In most cases, the development of adipocere is partial and irregular, and it is somewhat uncommon for the entire body to be affected. It may coexist with putrefactive decomposition. It is the result of hydrolysis and hydrogenation of adipose tissue (subcutaneous fat, intraperitoneal fat and retroperitneal fat), leading to the formation of the waxy substance consisting of fatty acids and calcium soaps. After months to years, adipocere becomes brittle and chalky. Adipocere formation requires certain environmental conditions—immersion in water and incarceration in wet graves or damp vaults potentiate the formation of adipocere; however, it has also been observed in dry concealment.[8,11–13] Adipocere is relatively well visualized on post-mortem CT imaging as sites of calcifications develop in hydrolysed fat although this may not be present in the early stages of adipocere formation. Such calcification appears as voids on post-mortem MRI and therefore proves difficult to identify.[14]

Mummification is the third type of long-term change after death which is the drying of tissues instead of liquefying putrefaction. It can coexist with other types of decomposition and requires a dry and, usually, warm environment where microbial activity is limited.[8,12] It can occur in freezing

Figure 11. Axial post-mortem CT image through the superior mediastinum of a young adult male who sustained severe blunt polytrauma with severe blood loss in the short antemortem interval between the index trauma and death. There is marked attenuated calibre of the arch of the aorta (arrow) (as well as of the remainder of the aorta and other great vessels—not shown).

Figure 12. Axial post-mortem CT image of the brain in an elderly female patient with known dementia. There is loss of the normal grey–white matter differentiation as a result of normal post-mortem fluid redistribution and autolysis. The mild early putrefactive gas changes are demonstrated (white arrows). The hyperdensity in the dural venous sinuses posteriorly (black arrows) is a normal post-mortem-dependent lividity appearance and should not be misinterpreted as pathological acute subdural haemorrhage or pathological dural venous sinus thrombosis. Note the chronic frontotemporal lobar degenerative brain parenchymal features in keeping with the antemortem diagnosis of frontotemporal dementia.

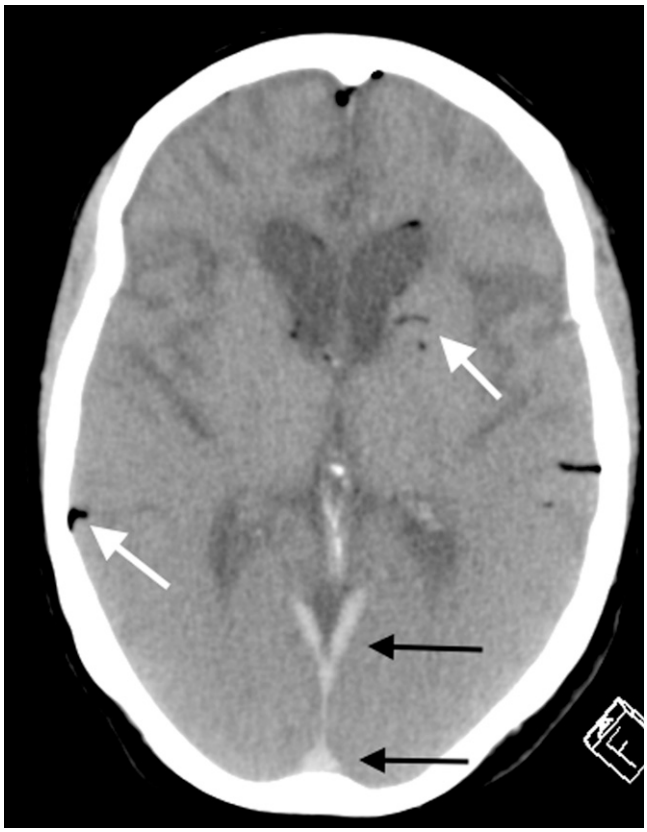

conditions, partly as a result of the dryness of the air and, again, partly because of the inhibition of bacterial activity. The key factor in mummification seems to be the evaporation of water from the body surface in dry conditions. Both adipocere formation and mummification preserve surface wounds which may be useful in forensic evaluation; however, putrefactive decomposition occurs more rapidly at sites where bacteria have been introduced into the body by the injury (or by insects).[8,11]

SITE-SPECIFIC POST-MORTEM CT CHANGES

Post-mortem hyperdensity of the aortic wall

Atherosclerosis can be readily appreciated on post-mortem imaging as well as antemortem imaging, particularly where there is significant calcification associated with such change. Hyperdensity of the aortic wall can also be observed in severe anaemia and aortic dissection in antemortem cross-sectional imaging. However, such hyperdensity may also be frequently observed as a non-pathological "normal" entity on post-mortem CT imaging and is presumed to be the result of a combination of: (1) contraction and collapse of the aortic wall secondary to loss of perfusion (pulsation) pressure with the resultant loss of vessel wall tension, (2) a lack of motion artefact and (3) post-mortem changes of blood sedimentation and separation within the vessel lumen into a cellular–serous fluid–fluid level because of stasis (*i.e.* intravascular hypostasis) (Figure 10).[15,16]

Post-mortem dilatation of the right atrium, superior vena cava and inferior vena cava

A degree of dilatation of the right atrium and concomitant prominence of the superior and inferior vena cavae may be observed on post-mortem cross-sectional imaging when adequate blood volume is present at the time of death.[17] This is in contradistinction to patients and victims in whom severe blood volume loss was a primary cause of death—in such cases, notable loss of calibre and cross-sectional area will be observed in relation to the cardiac chambers and the great vessels (vena cavae and aorta)—termed "the empty heart phenomenon" by the lead author (Figure 11).

Post-mortem cerebral fluid redistribution

In the post-mortem period, gradual mild loss of the normal grey–white matter differentiation becomes discernible on post-mortem CT imaging with the absence of any appreciable cerebral swelling (Figure 12). This is the result of fluid shifts within the brain parenchyma which have similar appearances to the true cerebral oedema observed in antemortem brain imaging following, for example, trauma or hypoxic ischaemic encephalopathy. This, however, is a normal post-mortem phenomenon and should not be misinterpreted as a direct consequence of perimortem hypoxic ischaemic encephalopathy.

Figure 13. Axial post-mortem CT image through the thorax of an adult male patient who underwent cardiopulmonary resuscitation attempts and was scanned soon after death. There is some gas in the anterior non-dependent aspect of the right atrium (arrow) with notable absence of decomposition change elsewhere on the post-mortem CT imaging. This distribution of gas is a common finding in subjects who underwent significant cardiopulmonary resuscitation efforts, particularly when there is no alternative imaging indication of putrefactive change.

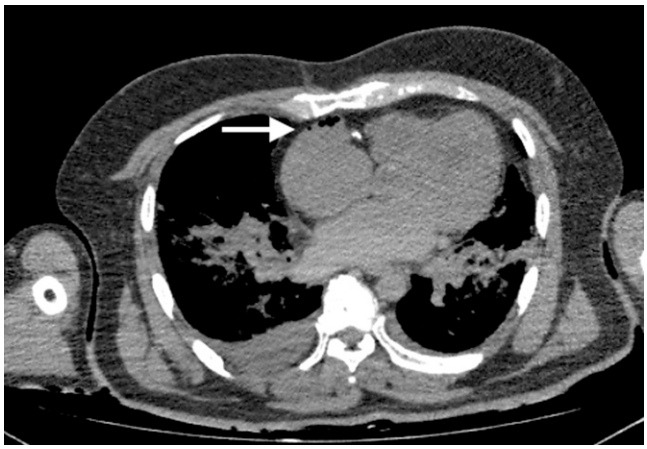

Figure 14. Axial post-mortem CT image through the abdomen of an adult male who underwent significant cardiopulmonary resuscitation attempts. Hepatic venous gas is demonstrated (arrow). The subject was imaged very soon after failed resuscitation, and there was no significant putrefactive change evident at the time of the post-mortem CT scan.

POST-MORTEM IMAGING FEATURES RELATED TO CARDIOPULMONARY RESUSCITATION

Some of the common post-mortem changes related to cardiopulmonary resuscitation exhibit features similar to some of those seen in association with post-mortem decomposition but are distinct entities.

Cardiovascular and abdominal visceral intravascular gas

There is a positive correlation between the presence of gas locules within the cardiac chambers and hepatic portal venous vessels on post-mortem imaging and preceding efforts of cardiopulmonary resuscitation. Cardiovascular gas may be identified not only in the cardiac chambers (Figure 13) (particularly in the non-dependent right ventricle) but also in the large venous vessels (the vena cavae, subclavian and brachiocephalic veins and the hepatic veins) (Figure 14). It is proposed that the origin of such gas occurring within the vascular tree is the result of the inflow of air secondary to medical venous cannulation and catheterization, pneumatization of dissolved gas within the blood as a result of cardiac massage (chest compressions), pulmonary parenchymal injury as a result of cardiopulmonary resuscitation or a combination of these mechanisms.[16–20] During cardiopulmonary resuscitation, the gas which has reached the described venous structures ascends or descends in a retrograde fashion (for example, to the brain or liver). On post-mortem imaging assessment, because cardiopulmonary resuscitation has not been successful and antegrade venous flow has not been reinstated, the intravascular gas is not carried away from these veins. The presence of gas within the portohepatic venous system on post-mortem imaging following cardiopulmonary resuscitation is therefore distinct from but may coexist with post-mortem putrefactive decomposition change; it should also be distinguished from imaging features secondary to genuine pathological processes such as bowel necrosis or ischaemia and intra-abdominal sepsis. In addition, such changes should not be misinterpreted as pathological air embolus in which the distribution of gas on post-mortem imaging is different.

Gaseous distension of the gastrointestinal tract

When artificial respiration has been performed through a bag-valve-mask resuscitator or oropharyngeal airway tube in the absence of endotracheal or nasotracheal intubation, the gastrointestinal tract may become distended with air which will be readily appreciated on post-mortem CT and MRI. Alternatively, inadvertent pharyngo-oesophageal intubation as a result of malpositioned endotacheal or nasotracheal tubes may cause similar post-mortem cross-sectional imaging appearances. However, a direct relationship between gaseous distension of the gastrointestinal tract and cardiopulmonary resuscitation has also been demonstrated

Figure 15. (a) Axial post-mortem CT image through the abdomen of an adult male who underwent significant cardiopulmonary resuscitation efforts. Bilateral relatively symmetrical anterior (or anterolateral) rib fractures (arrows) are very common in the adult population when effective chest compressions have been undertaken as part of cardiopulmonary resuscitation. Such fractures should not be misinterpreted as deliberate inflicted trauma. (b) Sagittal post-mortem CT (reformatted) image of a different adult male subject demonstrates a fracture of the mid-body of the sternum (arrow); the subject had undergone cardiopulmonary resuscitation with chest compressions; anterolateral rib fractures were also present (not shown).

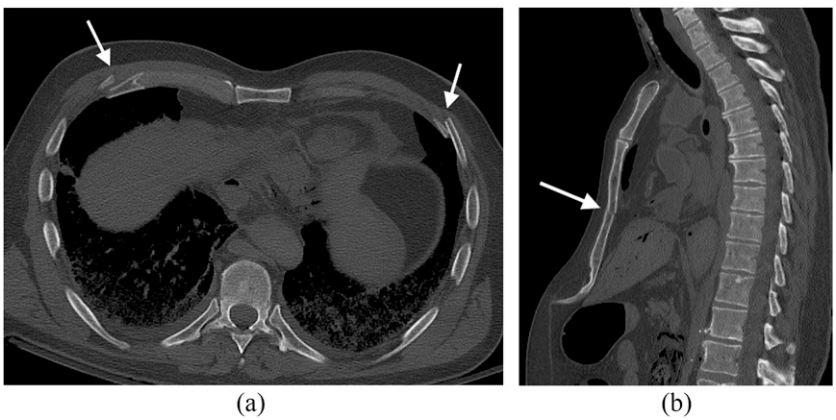

(a) (b)

and the extent of portoheaptic venous gas seems to correlate with the degree of gaseous distension.[19] This is distinct from the early post-mortem decomposition changes which may also be discernible as small and large bowel distension on post-mortem imaging. Such iatrogenic post-mortem imaging appearances should be borne in mind and distinguished from pathological processes such as ileus or mechanical gastrointestinal tract obstruction or bowel ischaemia.

Rib fractures

The chest compressions performed as part of cardiopulmonary resuscitation frequently cause rib fractures (Figure 15a) and, less frequently, sternal fractures (Figure 15b), particularly in the elderly.[21]

It can often be important to differentiate between such iatrogenic fractures secondary to cardiopulmonary resuscitation and traumatic fractures that might represent deliberate inflicted injuries, particularly in the elderly population (where physical elder abuse and neglect may be a coronial and safeguarding concern) and in the setting of suspicious deaths. In the author's experience, iatrogenic rib fractures secondary to cardiopulmonary resuscitation almost exclusively involve the second to eighth ribs bilaterally on post-mortem CT assessment and affect the anterolateral rib portion (including the costochondral junctions).

CONCLUSION

Familiarity with appropriate "normal" post-mortem changes on CT and MRI imaging as well as post-mortem imaging features presenting as a direct consequence of cardiopulmonary resuscitation is paramount to avoid erroneously attributing such appearances to a pathological or deliberate inflicted traumatic process.

REFERENCES

1. Maskell G, Wells M. *RCR/RCPath statement on standards for medico-legal post-mortem cross-sectional imaging in adults*. London, UK: RCR; 2012. Available from: https://www.rcr.ac.uk/sites/default/files/publication/FINAL-DOCUMENT_PMImaging_Oct12.pdf
2. *Chief Coroner Guidance No. 1. The use of post-mortem imaging (adults)*. 2013. Available from: http://www.judiciary.gov.uk/wp-content/uploads/JCO/Documents/coroners/guidance/guidance-no1-use-of-port-mortem-imaging.pdf
3. Kobayashi T, Isobe T, Shiotani S, Saito H, Saotome K, Kaga K, et al. Postmortem magnetic resonance imaging dealing with low temperature objects. *Magn Reson Med Sci* 2010; **9**: 101–8. doi: 10.2463/mrms.9.101
4. Tashiro K, Shiotani S, Kobayashi T, Kaga K, Saito H, Someya S, et al. Cerebral relaxation times from postmortem MR imaging of adults. *Magn Reson Med Sci* 2015; **14**: 51–6. doi: 10.2463/mrms.2013-0126
5. Kobayashi T, Shiotani S, Kaga K, Saito H, Saotome K, Miyamoto K, et al. Characteristic signal intensity changes on postmortem magnetic resonance imaging of the brain. *Jpn J Radiol* 2010; **28**: 8–14. doi: 10.1007/s11604-009-0373-9
6. Tofts PS, Jackson JS, Tozer DJ, Cercignani M, Keir G, MacManus DG, et al. Imaging cadavers: cold FLAIR and noninvasive brain thermometry using CSF diffusion. *Magn Reson Med* 2008; **59**: 190–5. doi: 10.1002/mrm.21456
7. Yen K, Anon J, Remonda L, Spreng A, Lovbland KO. Forensic neuroimaging. In: Thali MR, Dirnhofer R, Vock P, eds. *The virtopsy approach*. 1st edn. Boca Raton, FL: CRC Press; 2009. pp. 272–304.
8. Levy AD, Harcke HT, Mallak CT. Postmortem imaging: MDCT features of postmortem change and decomposition. *Am J Forensic Med Pathol* 2010; **31**: 12–17. doi: 10.1097/PAF.0b013e3181c65e1a
9. Shiotani S, Kohno M, Ohashi N, Yamazaki K, Itai Y. Postmortem intravascular high-density fluid level (hypostasis): CT findings. *J Comput Assist Tomogr* 2002; **26**: 892–3. doi: 10.1097/00004728-200211000-00006
10. Shiotani S, Kohno M, Ohashi N, Yamazaki K, Nakayama H, Watanabe K, et al. Non-traumatic postmortem computed tomographic (PMCT) findings of the lung. *Forensic Sci Int* 2004; **139**: 39–48. doi: 10.1016/j.forsciint.2003.09.016
11. Thali MJ, Yen K, Schweitzer W, Vock P, Ozdoba C, Dirnhofer R. Into the decomposed body-forensic digital autopsy using multislice-computed tomography. *Forensic Sci Int* 2003; **134**: 109–14. doi: 10.1016/S0379-0738(03)00137-3
12. Knight B. *Forensic pathology*. 2nd edn. London, UK: Arnold Publishing; 1996.
13. Swift B. Methods of time since death estimation within the early post-mortem interval. *J Homicide Major Incident Invest* 2010; **6**: 97–111.
14. Jackowski C, Thali M, Sonnenschein M, Aghayev E, Yen K, Dirnhofer R. Adipocere in postmortem imaging using multislice computed tomography (MSCT) and magnetic resonance imaging (MRI). *Am J Forensic Med Pathol* 2005; **26**: 360–4. doi: 10.1097/01.paf.0000188091.11225.38
15. Shiotani S, Kohno M, Ohashi N, Yamazaki K, Nakayama H, Ito Y, et al. Hyperattenuating aortic wall on postmortem computed tomography (PMCT). *Radiat Med* 2002; **20**: 201–6
16. Yamazaki K, Shiotani S, Ohashi N, Doi M, Honda K. Hepatic portal venous gas and hyper-dense aortic wall as postmortem computed tomography finding. *Leg Med (Tokyo)* 2003; **5**(**Suppl. 1**): S338–41.
17. Christe A, Flach P, Ross S, Spendlove D, Bolliger S, Vock P, et al. Clinical radiology and postmortem imaging (Virtopsy) are not the same: specific and unspecific postmortem signs. *Leg Med (Tokyo)* 2010; **12**: 215–22. doi: 10.1016/j.legalmed.2010.05.005
18. Shiotani S, Kohno M, Ohashi N, Atake S, Yamazaki K, Nakayama H. Cardiovascular gas on non-traumatic postmortem computed tomography (PMCT): the influence of cardiopulmonary resuscitation. *Radiat Med* 2005; **23**: 225–9.
19. Shiotani S, Kohno M, Ohashi N, Yamazaki K, Nakayama H, Watanabe K. Postmortem computed tomographic (PMCT) demonstration of the relation between gastrointestinal (GI) distension and hepatic portal venous gas (HPVG). *Radiat Med* 2004; **22**: 25–9.
20. Okuda T, Shiotani S, Kobayashi T, Kohno M, Hayakawa H, Kikuchi K, et al. Immediate non-traumatic postmortem computed tomographic demonstration of myocardial intravascular gas of the left ventricle: effects from cardiopulmonary resuscitation. *Springerplus* 2013; **2**: 86. doi: 10.1186/2193-1801-2-86
21. Hashimoto Y, Moriya F, Furumiya J. Forensic aspects of complications resulting from cardiopulmonary resuscitation. *Leg Med (Tokyo)* 2007; **9**: 94–9. doi: 10.1016/j.legalmed.2006.11.008